

Dark matter halo concentrations with a bayesian approach

Christian Poveda¹ & Jaime E. Forero-Romero¹

¹*Departamento de Física, Universidad de los Andes, Cra. 1 No. 18A-10, Edificio Ip, Bogotá, Colombia*

30 September 2014

ABSTRACT

asd

Key words: methods: numerical, galaxies: haloes, cosmology: theory, dark matter

1 INTRODUCTION

In the context of the concordance cosmology, the matter contents of the Universe are dominated by an unknown dark matter which behaves as a collisionless fluid only perturbed by gravity.

Numerical experiments are able to follow the non-linear evolution of dark matter down to galactic scales. On these scales a common approximation considers the matter distribution as spherical with a radial dependence. The function describing this distribution is known as a radial density profile.

The consensus is that density profiles are almost universal; almost independent of cosmological parameters and similar for different objects after some simple physical rescaling is applied.

The detailed halo structure influences the hosted galaxies.

The concentration parameter is important in galaxy formation studies.

Different studies vary about the result of the concentration-mass relationship.

We propose a new way to obtain the concentration for halos in N-body simulations.

We use the integrated mass profile because it allows us to use the data directly with the simulation without binning the particle positions and estimating a density.

As an application we study the mass concentration relationship.

(Navarro et al. 1997)

2 BASIC PROPERTIES OF THE NFW DENSITY PROFILE

The Navarro-Frenk-White density profile can be written as

$$\rho(r) = \frac{\rho_c \delta_c}{r/r_s (1 + r/r_s)^2}, \quad (1)$$

where $\rho_c \equiv 3H^2/8\pi G$ is the Universe critical density, δ_c is the halo dimensionless characteristic density and r_s is known as the scale radius, the radius that marks the transition between the two power law behaviour in the $\rho \propto r^{-1}$ for $r < r_s$ and $\rho \propto r^{-3}$ for $r > r_s$.

We define the virial radius of a halo, r_v , as the boundary of the spherical volume that encloses an average density of Δ_h times the average density of the Universe. The corresponding mass M_v , the virial mass, can be written as $M_v = \frac{4\pi}{3} \bar{\rho} \Delta_h r_v^3$.

2.1 Integrated Mass

From these definitions we can compute the total mass enclosed inside a radius r :

$$M(< r) = 4\pi \rho_c \delta_c r_s^3 \left[\ln \left(\frac{r_s + r}{r} \right) - \frac{r}{r_s + r} \right]. \quad (2)$$

We can now express the same quantity in terms of dimensionless the variables $x \equiv r/r_v$ and $m \equiv M(< r)/M_v$,

$$m(< x) = \frac{1}{A} \left[\ln(1 + xc) - \left(\frac{xc}{xc + 1} \right) \right], \quad (3)$$

where

$$A = \left[\ln(1 + c) - \left(\frac{c}{c + 1} \right) \right], \quad (4)$$

and the parameter c is known as the concentration $c \equiv r_v/r_s$.

The most interesting feature of Eq. (3) is that the concentration is the only free parameter to describe the density profile. In Figure 1 we show $m(< x)$ as a function of x for different values of the concentration in the range $1 \leq c \leq 20$.

2.2 Circular velocity

It is also customary to express the mass of the halo in terms of the circular velocity $V_c = \sqrt{GM(< r)/r}$. From this we can define a new dimensionless circular velocity $v(< x) \equiv V_c(< r)/V_c(< r_v)$, using the result in Equation 3 to have:

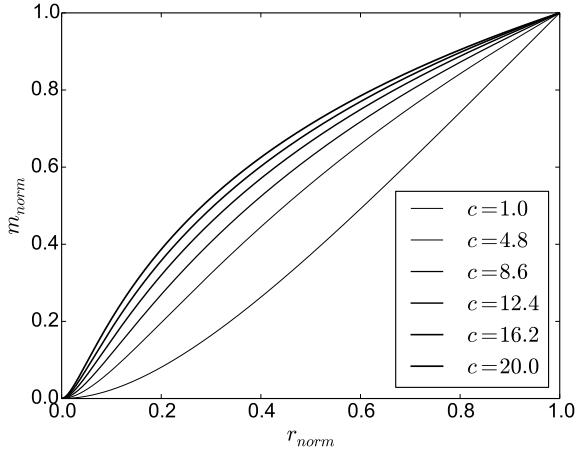


Figure 1. Dimensionless mass profiles as a function of the dimensionless radius for different concentration values.

$$v(< x) = \sqrt{\frac{1}{A} \left[\frac{\ln(1 + xc)}{x} - \frac{c}{xc + 1} \right]}, \quad (5)$$

In Figure XXX we show the circular velocity profile for the same concentrations as in Figure 1.

3 A NEW APPROACH TO HALO FITTING

We estimate the concentration parameter by fitting the integrated mass profile described in Equation (3). First we define the center of the halo to be at the position of the particle with the lowest gravitational potential.

We construct the integrated mass profile by ranking the particles by their increasing distance to the center of the halo. Once they are ranked, the total mass at a radius r_i , increases by m_p , where r_i is the position of the i -th particle and m_p is the mass of the computational particle. In this process we discard the particle at the center.

We stop the construction of the integrated mass profile once we arrive at an average density of $\Delta_h \bar{\rho}$, with $\Delta_h = 740$, roughly corresponding to 200 times the critical density. This radius marks the virial radius and the virial mass. We divide the total mass enclosed mass M_i and the radii r_i by these values to obtain the dimensionless variables x_i and m_i .

Using these new variables we define the following χ^2 function

$$\chi^2(c) = \sum_i [\log m_i - \log m(< x_i; c)]^2, \quad (6)$$

where $m(< x_i; c)$ corresponds to the values in Eq.(3) at $x = x_i$ for a given value of the concentration parameter c .

We sample the likelihood function distribution defined by $\mathcal{L}(c) = \exp(-\chi^2(c)/2)$ with a Metropolis-Hastings algorithms to find the optimum value of c and its associated uncertainty σ_c .

Cuántos pasos usa la cadena? De cuánto es el sigma en los saltos de c en la cadena?

Falta alguna figura que muestre resultados de la -log likelihood para algunos casos representativos.

4 HALO SAMPLES

We apply our method to two different halo samples. The first one is a mock sample to test the algorithm and asses the impact of the number of computational particles on the concentration values. The second sample comes from a publicly available N-body cosmological simulation. These results for these sample can be then compared against other methods to find the concentration and feed the discussion about the implications of our method.

4.1 Mock Halos

First, we test our method using mock halos with known values for the concentration. The method we use to generate the halos is based on the integrated mass profile. Given the number of particles n and the concentration c we define the mass element as $\delta m = 1/n$ (this corresponds to the mass of each particle such that the total mass is one). Then for each number k from 1 to n we find the value of r such that the difference

$$m(< r; c) - k \cdot \delta m \quad (7)$$

is zero using Ridders' method. This value of r is the radius of the k th particle of the generated halo, then polar and azimuthal angles θ and ϕ are randomly generated. Finally these three coordinates are transformed into cartesian coordinates $(r, \theta, \phi) \rightarrow (x, y, z)$. This process is repeated n times in order to generate the x, y, z coordinates for each particle.

We generate 100 mock halos with concentration values randomly placed in the range $1 < c < 20$. Each one of the halos is generated with four different total particle numbers: 20, 200, 2000 and 20000. This gives us a total of 500 halos.

4.2 Simulation Data

We use data from the MultiDark cosmological volume. This simulation follows the non-linear evolution of a dark matter density field sampled with 2048³ particles over a cubic box of $1000 h^{-1} \text{Mpc}$ on a side. The data is publicly available, more details about the structure of the database and the simulations can be found in (Riebe et al. 2013).

We select a sample of halos in a cubic sub-volume of $100 h^{-1} \text{Mpc}$ on a side centered on the most massive halo in the simulation at $z = 0$ ¹. We select first all the halos at $z = 0$ detected with a Friends-of-Friends (FoF) algorithm with masses in the interval $10^{11} \leq M_{\text{FoF}}/h^{-1} M_{\odot} \leq 10^{15}$. The FoF algorithm ran with a linking length of 0.17 times the average interparticle distance. This choice translates into an overdensity $\Delta_h \sim 400 - 700$ that is dependent on the halo concentration (More et al. 2011).

For each selected halo with the previous procedure we select from the database all the particles that belong to it. From the particles we follow the procedure spelled out in

¹ This corresponds to the miniMDR1 database in the MultiDark webpage

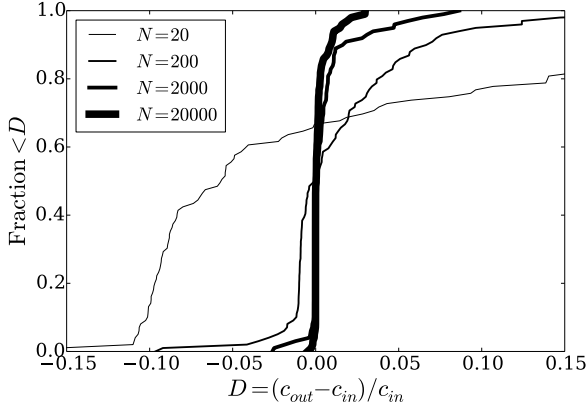


Figure 2. Cumulative distribution of the fractional difference between the input concentration in the mock halo generator, c_{in} and the measurement by our MCMC code, c_{out} . Each curve corresponds to halos generated with a different number of particles, N .

Section 3 with $\Delta_h = 740$ (corresponding to 200 times the critical density) to find the halo concentration. Finally, we store the values obtained for the virial radius, virial mass and concentration.

5 RESULTS

5.1 Mock Halos

In Figure 2 we show the integrated distribution percentual difference between the concentration measured with our fitting method c_{out} in comparison with the concentration used to generate the mock halos, c_{in} , $D = (c_{in} - c_{out})/c_{in}$. Then we can see that as the number of particles increases, the curve becomes more pronounced at 0. Showing that for most of the halos c_{in} is very similar to c_{out} .

5.2 Simulation Data

6 DISCUSSION

6.1 Comparison against other methods

We compared this method against two methods: The first one consists in using shells for estimating the density in function of the radius and using the same MCMC method for fitting and the second one consists in using the circular velocity $V(r) = \sqrt{GM(<r)/r}$ and the relation for the NFW profile

$$\frac{V_{max}}{V(r_v)} = \sqrt{\frac{0.216c}{M(r_v; c)}} \quad (8)$$

Where V_{max} is the maximum velocity, to find the value of the concentration. We tested the three methods using the same data from the Mock Halos test. In order to see the accuracy of each method depending on the number of particles we define

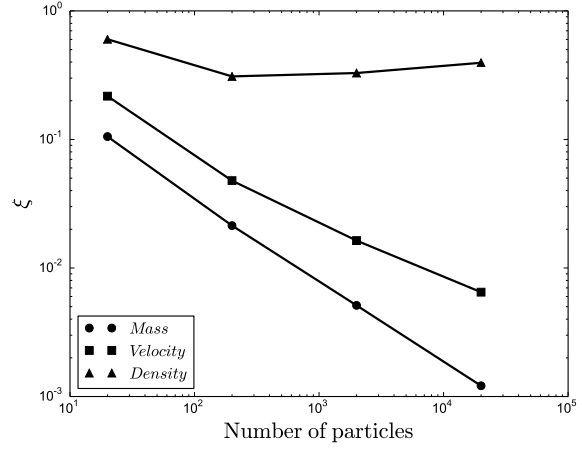


Figure 3. Relative error against number of particles

$$\xi(n) = \frac{1}{|\mathcal{H}_n|} \sum_{\mathcal{H}_n} \left| \frac{c_{org} - c_{obt}}{c_{org}} \right| \quad (9)$$

Where \mathcal{H}_n corresponds to the set of haloes with n particles, c_{org} and c_{obt} are the original and obtained concentrations respectively for each halo in \mathcal{H}_n and $|\mathcal{H}_n|$ the number of haloes in \mathcal{H}_n . Then we calculate ξ for each number of particles (20, 200, 2000 and 20000).

In Figure 3 we plotted ξ for the three methods. We consider that ξ is a good estimate because it is standardized, giving equal weight to all errors regardless of the magnitude of the concentrations or the number of haloes. On the other hand we have that ξ decreases quite fast with the number of particles for our method and is more precise in any case than the other methods. As mentioned in FIXME “for a large fraction of halos, and for the most massive in particular, the NFW functional does not Represent a good fit to the density profile.” This fact could explain why ξ increases with the number of particles for the density method.

We also used these three methods to obtain the concentration for each halo in miniMDR1 and compared the results. As can be seen in Figure 4 the three methods show mutually consistent results. However it can be inferred that the concentration values obtained by the method of circular velocity are higher than those obtained by our method, and also the values obtained by the density method are generally below the results of our method.

Running another test with halos whose concentrations vary as a normal distribution of variance σ^2 we found that the concentrations obtained by the method of circular velocity are a 35% greater than the ones obtained by the density method. However the concentrations obtained by the velocity method are barely higher (around 2% or 3%) than the ones obtained by our method. We did not find any significant variation in the concentration values obtained by any method by changing σ^2 in contrast with FIXME.

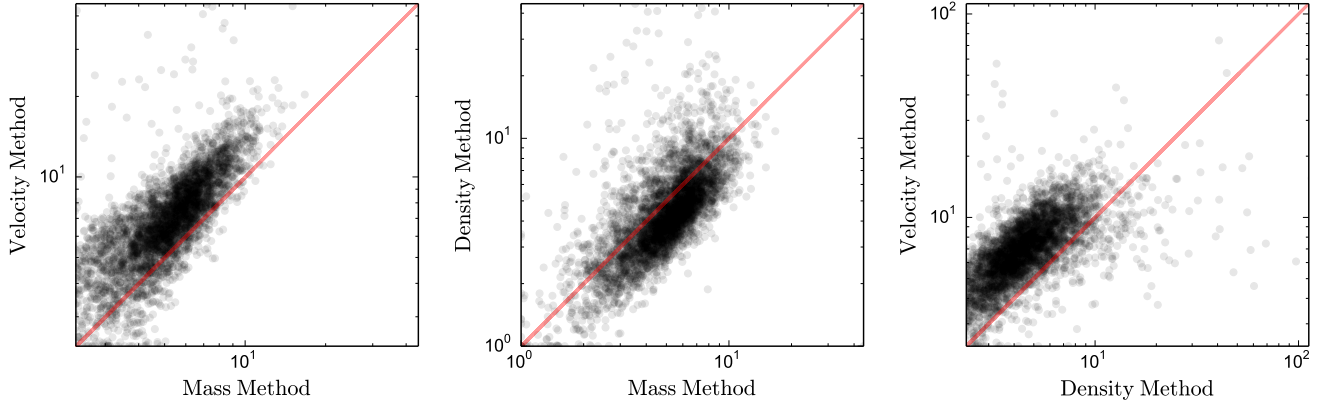


Figure 4. Comparison between the obtained concentrations by the three methods

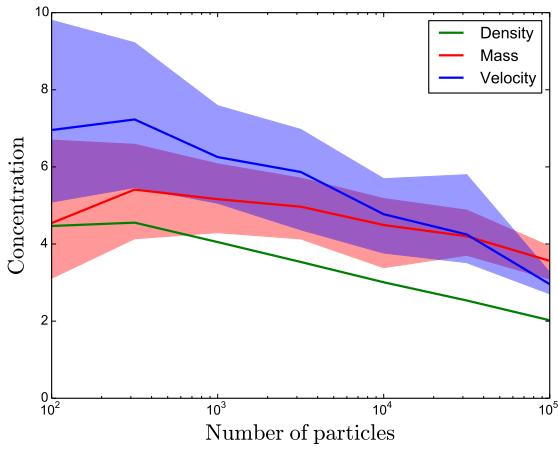


Figure 5. Concentration against number of particles

6.2 Concentration as a function of halo mass

Additionally we compared those three methods plotting the concentration as a function of the number of particles of each halo

The bold lines in Figure 5 corresponds to the median and the thinner lines corresponds to the quartiles. Showing that our method has values ranging from those obtained from the other two methods. Also we can see that the concentration obtained by the velocity method is higher than that obtained by the density method, this fact is consistent with FIXME.

6.3 Implication for comparisons against observations

FIXME: Ask to Jaime

7 CONCLUSIONS

FIXME: Ask to Jaime

REFERENCES

- More S., Kravtsov A. V., Dalal N., Gottlöber S., 2011, *ApJS*, 195, 4
 Navarro J. F., Frenk C. S., White S. D. M., 1997, *ApJ*, 490, 493
 Riebe K., Partl A. M., Enke H., Forero-Romero J., Gottlöber S., Klypin A., Lemson G., Prada F., Primack J. R., Steinmetz M., Turchaninov V., 2013, *Astronomische Nachrichten*, 334, 691